Performance Evaluation of An Automatic Segmentation Method of Cerebral Arteries in MRA Images By Use of Large Image Database

Yoshikazu Uchiyama[a], Tatsunori Asano[b], Takeshi Hara[b], Hiroshi Fujita[b], Yasutomi Kinosada[a], Takahiko Asano[c], Hiroki Kato[c], Masayuki Kanematsu[c], Hiroaki Hoshi[c], Toru Iwama[d]

[a]Dept. of Biomedical Informatics, Graduate School of Medicine, Gifu Univ., Japan
[b]Dept. of Intelligent Image Information, Graduate School of Medicine, Gifu Univ., Japan
[c]Dept. of Radiology, Graduate School of Medicine, Gifu University, Japan
[d]Dept. of Neurosurgery, Graduate School of Medicine, Gifu University, Japan

ABSTRACT

The detection of cerebrovascular diseases such as unruptured aneurysm, stenosis, and occlusion is a major application of magnetic resonance angiography (MRA). However, their accurate detection is often difficult for radiologists. Therefore, several computer-aided diagnosis (CAD) schemes have been developed in order to assist radiologists with image interpretation. The purpose of this study was to develop a computerized method for segmenting cerebral arteries, which is an essential component of CAD schemes. For the segmentation of vessel regions, we first used a gray level transformation to calibrate voxel values. To adjust for variations in the positioning of patients, registration was subsequently employed to maximize the overlapping of the vessel regions in the target image and reference image. The vessel regions were then segmented from the background using gray-level thresholding and region growing techniques. Finally, rule-based schemes with features such as size, shape, and anatomical location were employed to distinguish between vessel regions and false positives. Our method was applied to 854 clinical cases obtained from two different hospitals. The segmentation of cerebral arteries in 97.1% (829/854) of the MRA studies was attained as an acceptable result. Therefore, our computerized method would be useful in CAD schemes for the detection of cerebrovascular diseases in MRA images.

Keywords: Magnetic resonance angiography (MRA), Vessel segmentation, Large image database.

1. INTRODUCTION

Before the 1980's cerebrovascular diseases were first leading cause of death in Japan (Fig.1).[1] However, because of the progress in the medical treatment of hypertension, the number of cerebrovascular diseases has gradually decreased over the years. They are now the third leading cause of death in Japan. As shown in Fig.1(b), the main cause of this decrease in the number of cerebrovascular diseases is a reduction in cerebral hemorrhages. However, it should be noted that the numbers of cerebral infarctions and subarachnoid hemorrhages are increasing. Therefore, it is important to reduce the incidence of cerebral infarctions and subarachnoid hemorrhage. For the early detection of cerebral and cerebrovascular diseases, a screening system, called the *Brain Dock* or *Brain Check-up*, is widely employed in Japan. In this screening system, magnetic resonance imaging (MRI) is normally utilized. Because of recent developments in MRI, various types of cerebral diseases can be detected. Therefore, we developed computer-aided diagnosis (CAD) schemes for the detection of lacunar infarcts on T1- and T2-weighted images,[2–5] leukoaraiosis on T1- and T2-weighted images,[6] unruptured aneurysms in magnetic resonance angiography (MRA),[7–9] and occlusions in MRA images.[10]

Unruptured aneurysms are frequently identified by the abovementioned screening system. The detection and management of unruptured aneurysms are important because aneurysm rupture is the main cause of subarachnoid hemorrhage. However, it is difficult to detect small aneurysms in MRA images because of the overlap between the aneurysms and the adjacent vessels in a maximum-intensity projection (MIP) image. Therefore, several CAD schemes for the detection of unruptured aneurysms have been reported.[7,8,11–14] Since an automatic segmentation

Corresponding author information: E-mail uchiyama@gifu-u.ac.jp.

Medical Imaging 2009: Computer-Aided Diagnosis, edited by Nico Karssemeijer, Maryellen L. Giger
Proc. of SPIE Vol. 7260, 72602J · © 2009 SPIE · CCC code: 1605-7422/09/$18 · doi: 10.1117/12.811435

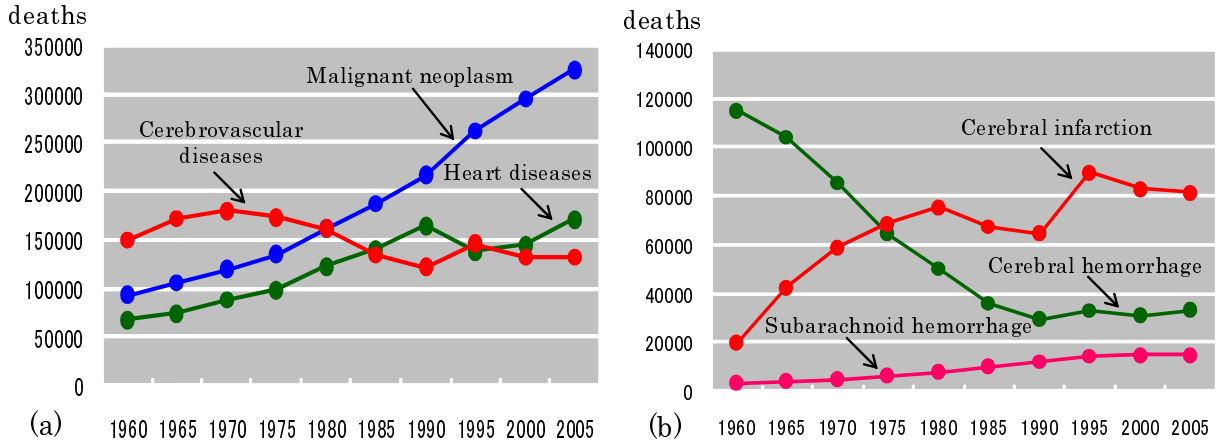

Figure 1. (a) Trend in leading causes of death in Japan. Cerebrovascular diseases are the third leading cause of death in Japan. (b) Trend in deaths from cerebrovascular diseases in Japan. The numbers of cerebral infarctions and subarachnoid hemorrhages are increasing.

method for cerebral arteries is an essential component of these CAD scheme, several methods have been reported so far. However, these methods have problems, i.e., (1) they are time consuming and (2) their performance were evaluated using small image datasets.

This paper describes a practical method for the segmentation of cerebral arteries in MRA images based on thresholding and region growing techniques. In addition, we evaluated our method using a large image dataset.

2. MATERIAL

A database consisting of 854 MRA studies was obtained from two different hospitals. 372 of these MRA studies were acquired on a 1.5 T magnetic image scanner (a Signa Excite Twin Speed 1.5 T; GE Medical Systems) at the Kizawa Memorial Hospital (Minogamo, Japan). Each of these MRA studies included 76 to 100 slice images. The axial slice images had a fixed size of 256 $\times$ 256 pixels, and the size of the pixels ranged from 0.469 mm to 0.625 mm. The thickness of each slice was in the range of 0.6 mm to 0.8 mm. The remaining 482 MRA studies were performed using a 1.5 T magnetic image scanner (Symphony; SIEMENS) at Gero Hot Springs Hospital (Gero, Japan). Each of these MRA studies involved 72 to 80 slice images. The axial slice images had a size of either 256 $\times$ 192 or 256 $\times$ 176 pixels. The slice thickness of each slice was in the range of 0.7 mm to 1 mm. All of the MRA studies were conducted using a 3D time-of-flight technique. The acquired MRA data were subsequently converted to isotropic volume data by using linear interpolation. The size of the converted 3D volume data was 400 $\times$ 400 $\times$ 200 voxels, and the size of each voxel was 0.5 $\times$ 0.5 $\times$ 0.5 mm^3. The obtained isotropic volume data were employed in this study.

3. METHOD

3.1 Gray scale transformation

Our dataset was comprised of MRA images obtained from two different hospitals. These images were acquired under different conditions. Therefore, the signal intensities of the vessel regions were different in each of the MRA images. Fig.2 shows two images obtained from the two hospitals. As shown in the histograms of these images, it is difficult to segment the vessel regions using a fixed threshold value. To overcome this issue, a gray-level transformation was applied to the 3D MRA image so that the minimum voxel value became zero, and voxels with values greater than the 99% margin depicted in a cumulative histogram were assigned a maximum value of

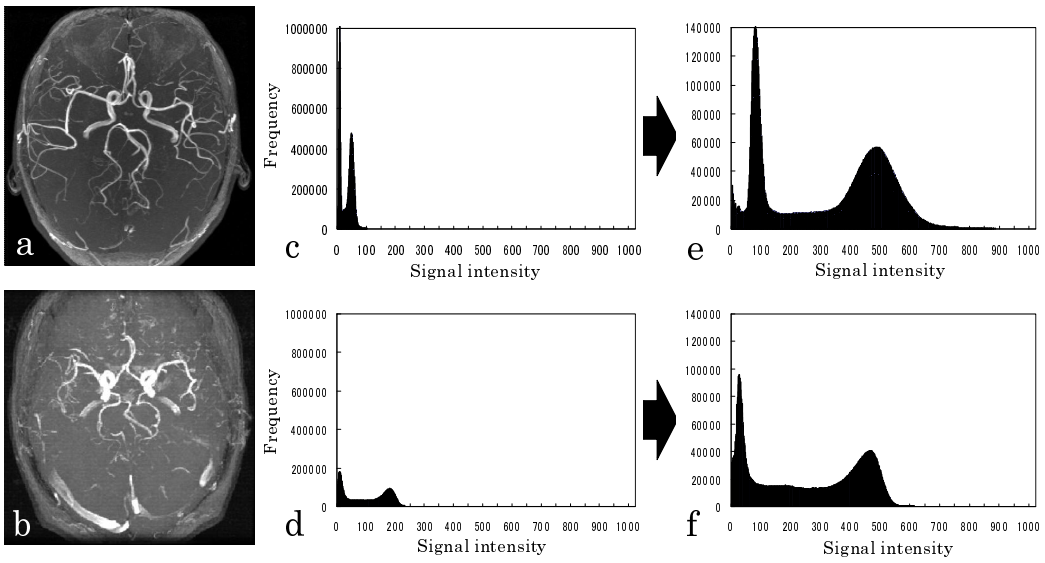

Figure 2. Examples of MRA images obtained from two hospitals. (a) and (b) are MIP images of 3D MRA images. (c) and (d) are the histograms of (a) and (b), respectively. As shown in these histograms, the signal intensities are different in the two MRA images. (e) and (f) are the histograms obtained by using a gray scale transformation, respectively.

1024. The gray scale transformation was defined by

$$\begin{cases} f'(i,j) = & \dfrac{1024-0}{C-0}(f(i,j)-0), & \text{for } f(i,j) \le C \\ f'(i,j) = & 1024, & \text{for } C < f(i,j) \end{cases}$$

where $f(i,j)$ and $f'(i,j)$ are an original image and a new image, respectively. C is the pixel value of 99% in the cumulative histogram obtained from the original image. As shown in the histograms of Fig.2(e) and Fig.2(f), the extraction of vessel regions was made easy by using a simple thresholding technique.

3.2 Adjustment of variations in the patient positioning

Fig.3 shows two MRA images acquired at the Gero Hot Springs Hospital and Kizawa Memorial Hospital. As shown in these figures, there was a difference due to variations in the positioning of the patients. The location information is a useful feature for the segmentation of cerebral arteries. Thus, we adjusted the location by using an image registration technique. To reduce the computation time, we made 2D MIP images from the 3D MRA images and determined a translation vector $T(x,y)$ in the 2D MIP image. We first selected a reference image from our database and manually cut out a rectangular region that included vessel regions in the 2D MIP image. The rectangular image was used as a template. By using the 2D template image and a 2D MIP image of the target 3D MRA image, we calculated a corresponding point for the image registration. The similarity between the vessel regions in a template image and the vessel regions in a target image was obtained by

$$D(x,y) = \sum_{i=0}^{m-1}\sum_{j=0}^{n-1} |f_t(i,j) - f_w(i+x, j+y)|,$$

where $x = 0, \cdots, M-m+1$ and $y = 0, \cdots, N-n+1$ when the template is $m \times n$ pixels. The image is$M \times N$ pixels, f_t shows the template, and f_w is the window in the target image being matched to the template. Position (x,y) shows the position of the template in the target image. By changing x and y, the template is shifted in the image and at each shift position the sum of the absolute differences between the corresponding pixels in the template and window is determined. This metric actually measures the dissimilarity between the template and the window. The smaller the D, the more similar will be the template and window. We used a sequential

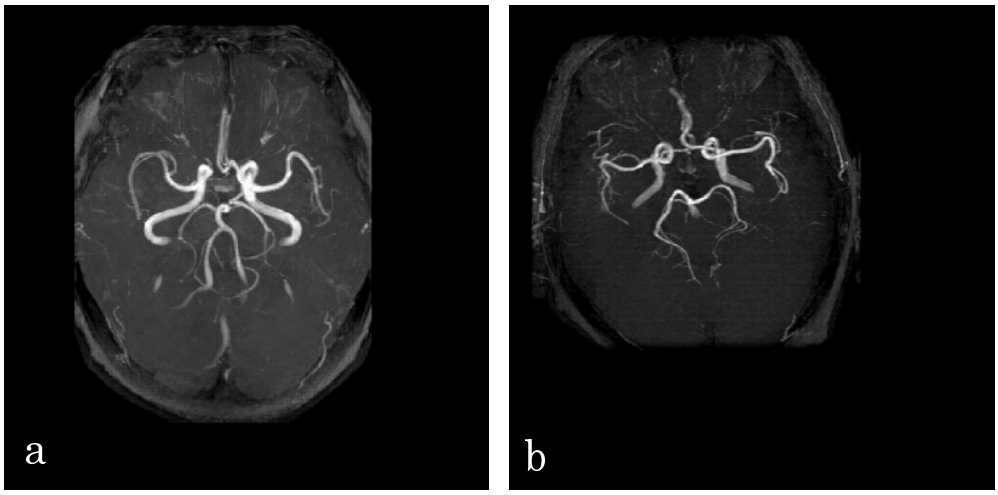

Figure 3. (a) Example of MRA image acquired at Gero Hot Springs Hospital. (b) Example of MRA image acquired at Kizawa Memorial Hospital. These images are MIP images of 3D MRA. The differences due to variations in the positioning of the patients are shown in these images.

similarity detection algorithm (SSDA).[15] This method reduced the computation time by stopping the process when the sum reached a value larger than a previously reached value, since the search was for the smallest sum. By using the corresponding point, the target MRA images were shifted into a common coordinate. The adjusted locations in a common coordinate were a useful feature for the segmentation of vessel regions.

3.3 Extraction of the vessel regions

After the gray-level transformation, the vessel regions were segmented from the background by using a gray-level thresholding method with a threshold level of 700, which was selected empirically. Using this method, large vessels regions were successfully segmented. However, it was difficult to segment small vessels using this method because the voxel values in the small vessel regions were low. Therefore, a region growing technique was subsequently applied to segment the small vessel regions. In this region growing technique, initial seed points were given as the segmented large vessel regions. The region was grown by appending to each seed point those neighboring voxels that had a value greater than 500. The growth of the region was stopped when no more voxels satisfied the criteria.

3.4 Elimination of false positives

Using the techniques described in the previous section, most of the vessel regions were segmented accurately. However, the candidate regions initially selected also included many false positives (FPs). To eliminate these, we determined the x and y locations and the volume of each candidate region.

Location. - The x and y locations were defined based on the center of gravity in a candidate region. By using the method described in Section 3.2, cerebral arteries were located at the central region. Thus, candidates on the periphery of the cerebral regions had a strong possibility of being FPs. Based on the location, these candidates could be eliminated as FPs.

Volume. - The volume was defined by the number of voxels in a candidate region, because vessel regions have a large volume. Therefore, candidates that had a small volume could be eliminated as FPs.

The rule-based scheme with 3 features was employed for the elimination of FPs. Fig.4 shows the result of eliminating FPs. As shown in these figures, image features related to the location and size were useful for eliminating FPs.

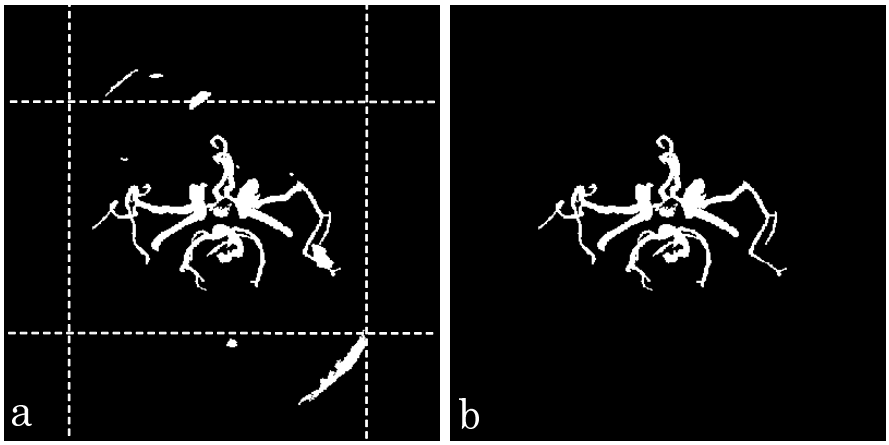

Figure 4. Example of elimination of FPs. (a) The resulting image from a region growing technique. Some over segmented regions are shown in this image. (b) The resulting image from the elimination of FPs. The dotted lines indicate the thresholds for the x and y locations. By using three features, e.g., the x and y locations, and the size, many FPs can be eliminated.

3.5 Performance evaluation

It was difficult to identify the voxels of vessel regions in each slice of a 3D MRA image, because the signal intensities within small vessel regions had low values. Therefore, we evaluated the results by using 2D MIP images. The performance of the segmentation algorithm could be assessed by comparing the computer-segmented regions to regions drawn by human observers. The overlap between the computer segmentation and manual segmentation was given by

$$O = \frac{Area(M \bigcap C)}{Area(M \bigcap C)},$$

where M is the manually segmented regions and C is the computer-segmented regions. The overlap ranged between zero and one, being zero in the case of no overlap and one in the case of an exact overlap.

It was difficult to manually segment the vessel regions in all 854 cases. We also employed a subjective rating using the MIP image. We used a three-point scale as described in the following. (1) Poor: most of the cerebral arteries were not well segmented, (2) Fair: most of the vessel regions were well segmented but with some minor errors, and (3) Good: all of the vessel regions were perfectly segmented.

4. RESULTS AND DISCUSSIONS

We selected 25 cases from the image datasets acquired at Kizawa Memorial Hospital (Kizawa DB), and 25 cases from the image datasets acquired at Gero Hot Springs Hospital (Gero DB). We manually segmented vessel regions in a total of 50 cases. The performance of the segmentation algorithm was assessed by using the overlap values described in Section 3.5. The overlap results for the Kizawa DB and Gero DB were 0.878 and 0.859, respectively. The overlap result for the 50 datasets was 0.869.

For the subjective evaluation, the proposed method was applied to 854 clinical cases obtained from two different hospitals. Table 1 shows the subjective rating results for the entire image database. The results obtained for the Kizawa DB showed that 197 (40.9%) cases were rated good, 267 (55.4%) cases were rated fair, and 18 (3.7%) cases were rated poor, respectively. On the other hand, the results obtained for the Gero DB showed that 134 (36.0%) cases were rated good, 231 (62.1%) cases were rated fair, and 7 (1.9%) cases were rated poor. Fig.5 shows examples of the good, fair, and poor segmentation results. In a fair segmentation result, some small vessel regions were not segmented accurately. However, this posed no problem for the application to the automatic detection of unruptured aneurysms in MRA images, because unruptured aneurysms cannot be found in such small vessel regions. The results rated good or fair were considered acceptable and would be adequate

	Good	Fair	Poor	Sum
Kizawa DB	197 (40.9%)	267 (55.4%)	18 (3.7%)	482
Gero DB	134 (36.0%)	231 (62.1%)	7 (1.9%)	372

Table 1. The results for the automatic segmentation of vessel regions for the entire image database.

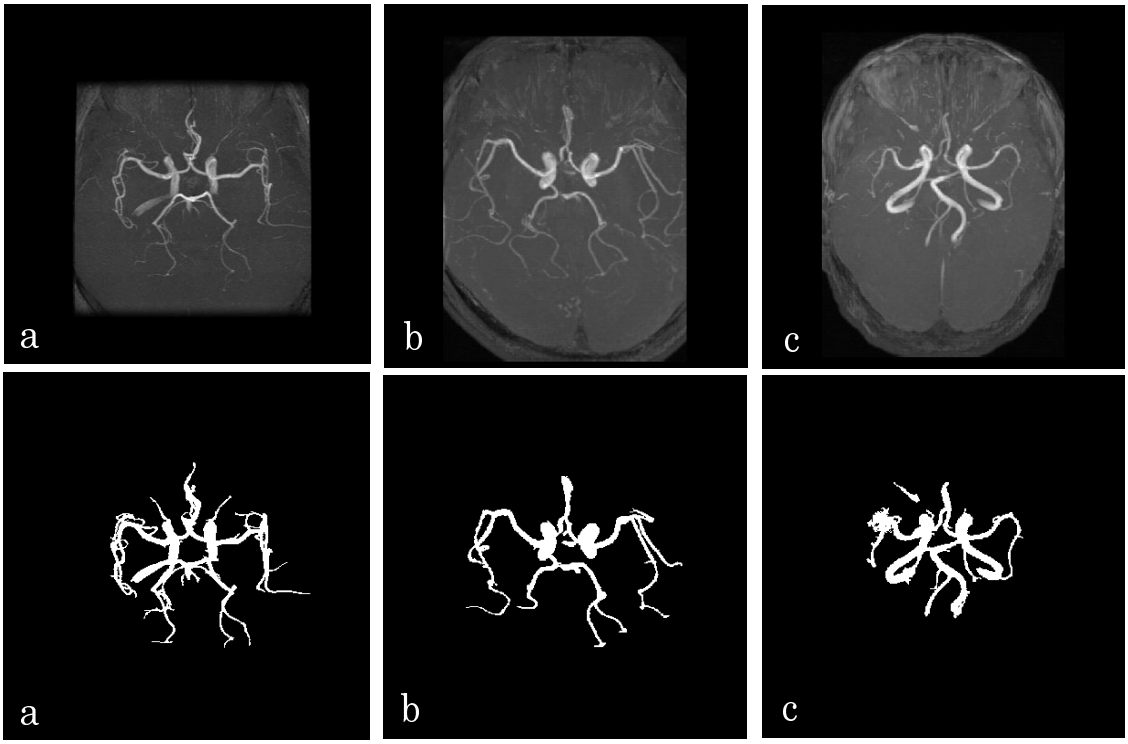

Figure 5. The images and results of vessel segmentation. The upper images are the original images. The bottom images are the result images. (a) Good segmentation result. (b) Fair segmentation result. (c) Poor segmentation result.

for clinical use. Overall, the segmentation of vessel regions in 97.1% (829/854) of the MRA studies attained a clinically acceptable result.

5. CONCLUSIONS

We developed a computerized method for segmenting cerebral arteries in MRA images. The results of experiment that used a large image database indicated that 97.1% (829/854) of the MRA studies achieved acceptable segmentation results. Therefore, our computerized method would be useful for the segmentation of vessel regions in MRA images.

ACKNOWLEDGMENTS

This work was partly supported by a grant for the Knowledge Cluster Creation Project from the Ministry of Education, Culture, Sports, Science and Technology, Japan. The authors thank the staffs in the Department of

Radiology and Neurosurgery at Kizawa Memorial Hospital and the staffs in the Department of Radiology and Neurosurgery at Gero Hot Springs Hospital for collecting image data.

REFERENCES

1. Statistics and information department minister's secretariat ministry of health labour and welfare Japan (eds), *Vital Statistics of Japan*, Health and Welfare Statistics Association, Tokyo, 2005.
2. R. Yokoyama, X. Zhang, Y. Uchiyama, H. Fujita, T. Hara, X. Zhou, M. Kanematsu, T. Asano, H. Kondo, S. Goshima, H. Hoshi, and T. Iwama, "Development of an automated method for detection of chronic lacunar infarct regions on brain MR images," *IEICE Trans. Inf. Syst.* **E90-D(6)**, pp. 943–954, 2007.
3. Y. Uchiyama, R. Yokoyama, H. Ando, T. Asano, H. Kato, H. Yamakawa, H. Yamakawa, T. Hara, T. Iwama, H. Hoshi, and H. Fujita, "Computer-aided diagnosis scheme for detection of lacunar infarcts on MR image," *Academic Radiology* **14(12)**, pp. 1554–1561, 2007.
4. Y. Uchiyama, R. Yokoyama, H. Ando, T. Asano, H. Kato, H. Yamakawa, H. Yamakawa, T. Hara, T. Iwama, H. Hoshi, and H. Fujita, "Improvement of automated detection method of lacunar infarcts in brain MR images," *Proc of IEEE Engineering in Medicine and Biology 29th Annual International Conference* **1**, pp. 1599–1602, 2007.
5. Y. Uchiyama, T. Kunieda, T. Asano, H. Kato, T. Hara, M. Kanematsu, T. Iwama, H. Hoshi, Y. Kinosada, and H. Fujita, "Computer-aided diagnosis scheme for classification of lacunar infarcts and enlarged virchow-robin spaces in brain MR image," *Proc of IEEE Engineering in Medicine and Biology 30th Annual International Conference* **1**, pp. 3908–3911, 2008.
6. Y. Uchiyama, T. Kunieda, T. Hara, H. Fujita, H. Ando, H. Yamakawa, T. Asano, H. Kato, T. Iwama, M. Kanematu, and H. Hoshi, "Automatic segmentation of different-sized leukoaraiosis regions in brain MR images," *Proc. of SPIE Medical Imaging : Computer-Aided Diagnosis* **6915**, pp. 69151S–1–69151S–8, 2008.
7. Y. Uchiyama, H. Ando, R. Yokoyama, T. Hara, H. Fujita, and T. Iwama, "Computer-aided diagnosis scheme for detection of unruptured intracranial aneurysms in MR angiography," *Proc of IEEE Engineering in Medicine and Biology 27th Annual International Conference* **1**, pp. 3031–3034, 2005.
8. Y. Uchiyama, X. Gao, T. Hara, H. Fujita, H. Ando, H. Yamakawa, T. Asano, H. Kato, T. Iwama, M. Kanematu, and H. Hoshi, "Computerized detection of unruptured aneurysms in MRA images: Reduction of false positives using anatomical location feature," *Proc. of SPIE Medical Imaging : Computer-Aided Diagnosis* **6915**, pp. 69151Q–1–69151Q–8, 2008.
9. Y. Uchiyama, M. Yamauchi, H. Ando, R. Yokoyama, T. Hara, H. Fujita, T. Iwama, and H. Hoshi, "Automated classification of cerebral arteries in MRA images and its application to maximum intensity projection," *Proc of IEEE Engineering in Medicine and Biology 28th Annual International Conference* **1**, pp. 4865–4868, 2006.
10. M. Yamauchi, Y. Uchiyama, R. Yokoyama, T. Hara, H. Fujita, H. Ando, H. Yamakawa, T. Iwama, and H. Hoshi, "Computerized scheme for detection of arterial occlusion in brain MRA images," *Proc. of SPIE Medical Imaging : Computer-Aided Diagnosis* **6514**, pp. 65142C–1–65142C–9, 2007.
11. H. Arimura, Q. Li, Y. Korogi, T. Hirai, H. Abe, Y. Yamashita, S. Katsuragawa, R. Ikeda, and K. Doi, "Automated computerized scheme for detection of unruptured intracranial aneurysms in three-dimensional MRA," *Academic Radiology* **11**, pp. 1093–1104, 2004.
12. H. Arimura, Q. Li, Y. Korogi, T. Hirai, S. Katsuragawa, Y. Yamashita, K. Tsuchiya, and K. Doi, "Computerized detection of intracranial aneurysms for three-dimensional mr angiography: Feature extraction of small protrusions based on a shape-based difference image technique," *Medical Physics* **33**, pp. 394–401, 2006.
13. H. Hayashi, Y. Masutani, T. Matsumoto, H. Mori, A. Kunimatsu, O. Abe, S. Aoki, K. Ohtomo, N. Takano, and K. Matsumoto, "Feasibility of a curvature-based enhanced display system for detecting cerebral aneurysms in MR angiography," *Magnetic Resonance in Medical Science* **2**, pp. 29–36, 2003.
14. S. Kobayashi, K. Kondo, and Y. Hata, "Computer-aided diagnosis of intracranial aneurysms in MRA images with case-based reasoning," *IEICE Trans. Info. Syst.* **E89-D(1)**, pp. 340–350, 2006.
15. D. I. Barnea and H. F. Silverman, "A class of algorithms for fast digital image registration," *IEEE Trans. Comput.* **C-21(2)**, pp. 179–186, 1972.